Lattice Vibration Spectra XXIV *

Far-Infrared Reflection Spectra, Optical and Dielectric Constants, and Effective Charges of the Pyrite Type Compounds FeS_2, MnS_2, $MnSe_2$, and $MnTe_2$

H. D. Lutz *, G. Kliche, and H. Haeuseler

Laboratorium für anorganische Chemie der Universität Siegen

Z. Naturforsch. **36a**, 184–190 (1981); received December 8, 1980

From the far-infrared reflection spectra of the pyrite type compounds FeS_2, MnS_2, $MnSe_2$, and $MnTe_2$ we determined the TO and LO phonon frequencies at wave vector $|q| \approx 0$ by both Kramers-Kronig analysis and classical oscillator fit method. In the case of $MnSe_2$ and $MnTe_2$ we found for the first time all five group-theoretically allowed reststrahlen bands. The phonon frequencies obtained from both single crystal and pressed pellet reflection measurements do not show any significant differences. The calculated optical and dielectric constants however are strongly affected by the surface quality of the sample. Effective ionic charges (Born effective charge, Szigeti charge) were calculated from the experimentally determined TO/LO splittings. They demonstrate an increasing ionicity in the order $FeS_2 < MnTe_2 < MnSe_2 < MnS_2$.

The transition metal dichalcogenides with pyrite structure form a wide class of compounds with complex and interesting physical properties. The chemical bonding in these materials depends mainly on the d-electron configuration of the metal atoms. Hence the ionicity of the bonds in pyrite type crystals can vary to a great extent [1].

For semiconducting members of the pyrite series, e.g. FeS_2, MnS_2, $MnSe_2$, and $MnTe_2$, both the ionicity, i.e. the effective charges [1–3], and the degree of covalency, shown by the short range forces [3–5], were calculated from the infrared optical data. These previous attempts of such investigations failed because of the lack of accurate frequencies, and despite a number of recent studies on the far-infrared properties of the pyrites [1–10] there are still important problems to be solved. Thus for most pyrites, viz. $MnSe_2$ and $MnTe_2$, not all predicted reststrahlen bands have been observed.

In this work we have analysed the far-infrared reflection spectra of the pyrites FeS_2, MnS_2, $MnSe_2$, and $MnTe_2$. From the optical and dielectric constants we wanted to obtain the full set of the transverse and longitudinal optical phonon frequencies (wave vector $|q| \approx 0$) with the help of both classical oscillator method and Kramers-Kronig analysis. From these data we intended to calculate the effective dynamical ionic charges of the atoms. We have further studied the question whether reflection data obtained from polycrystalline samples can be used for the calculation of correct phonon frequencies.

1. Experimental

MnS_2 was prepared from K_2S_x and freshly precipitated MnS in an autoclave as described elsewhere [6]. $MnSe_2$, $MnTe_2$, and FeS_2 were prepared by heating stoichiometric mixtures of the elements in evacuated quartz tubes at 380 ($MnSe_2$) and 600 °C ($MnTe_2$, FeS_2). It was difficult to obtain pure samples of $MnSe_2$, because $MnSe_2$ tends to decompose into MnSe + Se at higher temperatures [11].

X-ray analysis was used to confirm the structure and the lattice constants of the cubic dichalcogenides. The latter were found to be in good accordance with literature data.

Measurements of the reflectivity at near normal incidence were performed at room temperature with a Bruker IFS 114 Fourier-transform interferometer in the spectral range from 700 to 40 cm^{-1} and the grating spectrophotometer Perkin Elmer model 580 in the range from 1000 to 200 cm^{-1}. Highly polished faces of a natural specimen of FeS_2 were compared against an aluminium mirror as reference. From the powdered samples pellets with mirror like surfaces were obtained by pressing with a pressure of 10^4 bar at ambient temperature.

* XXIII. Communication: H. D. Lutz, G. Kliche, Z. anorg. allg. Chem., in press.

Reprint requests to Prof. Dr. H. D. Lutz, Universität Siegen, Adolf-Reichwein-Straße, D-5900 Siegen 21.

0340-4811 / 81 / 0200-0184 $ 01.00/0. — Please order a reprint rather than making your own copy.

2. Far-Infrared Reflection Spectra

Unit cell group analysis predicts five infrared active lattice vibration for pyrite-type compounds [6]:

$$\Gamma = A_g + E_g + 3T_g + 2A_u + 2E_u + 5T_u$$

(space group Pa3, $Z = 4$).

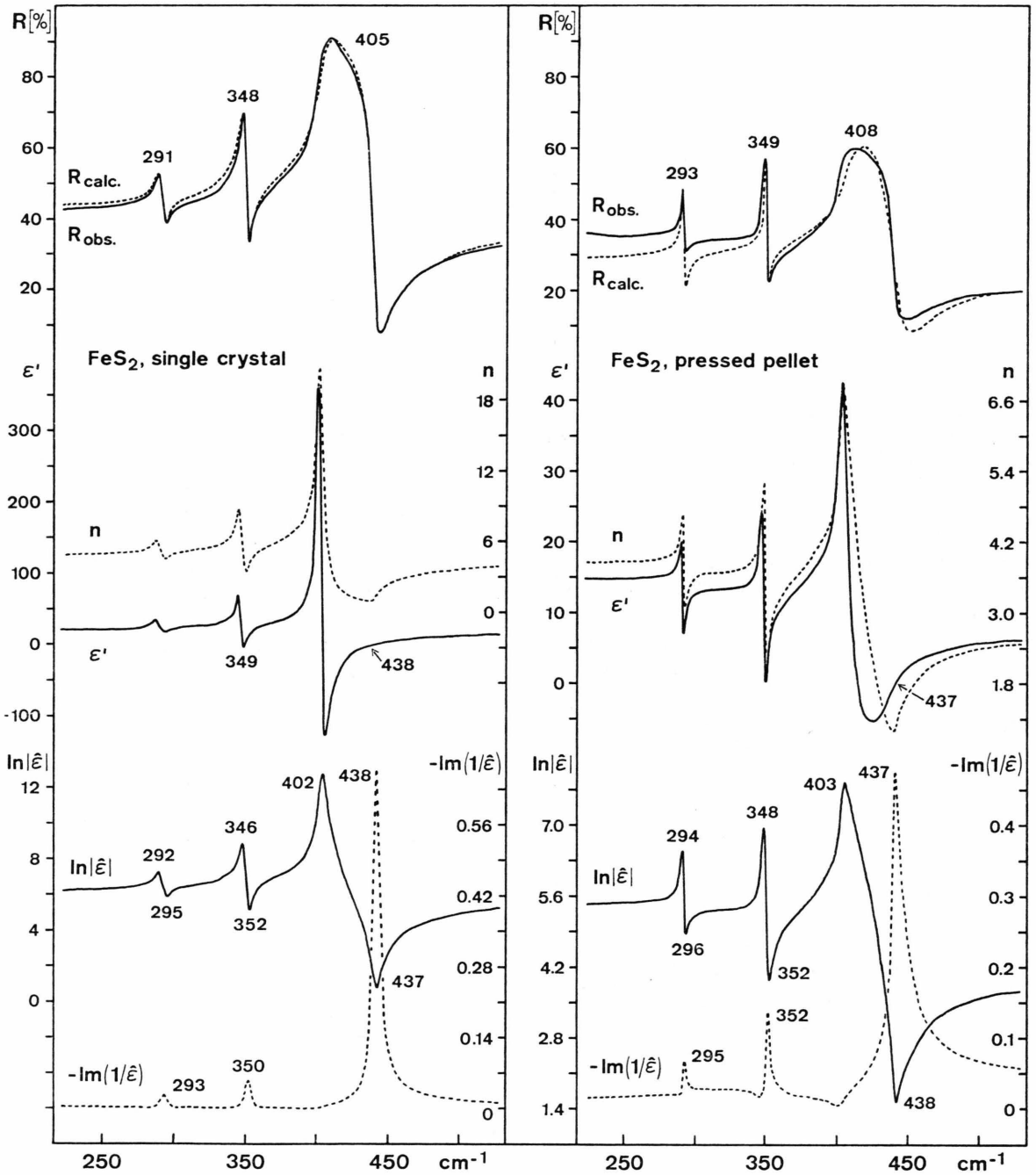

Fig. 1. FIR-reflection spectra, optical and dielectric constants (Kramers-Kronig analysis) of FeS_2 from single crystal (PE 580) and pressed pellet (Bruker IFS 114) measurements.

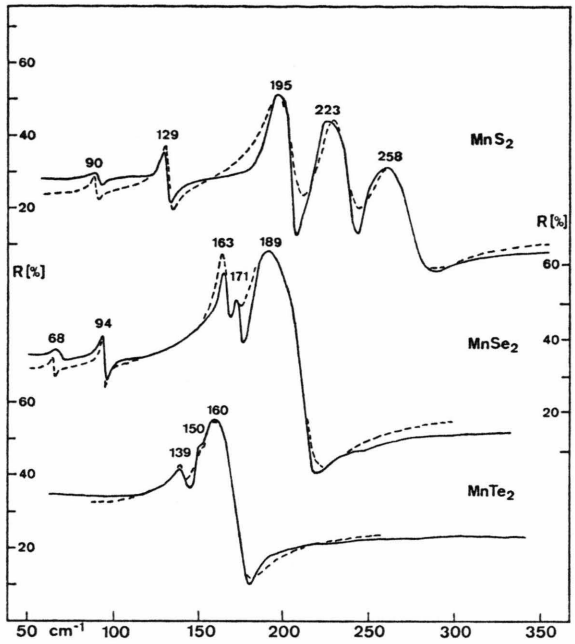

Fig. 2. FIR-reflection spectra (Bruker IFS 114) of the manganese dichalcogenides MnS_2, $MnSe_2$, and $MnTe_2$, full line; oscillator fit, dashed line.

Figures 1 and 2 show the reflection spectra of the pyrites under investigation.

Contrary to Verble and Humphrey [9], who observed only three reststrahlen bands for MnS_2, but in accordance with the formerly published absorption spectrum [6], we found five reststrahlen bands for MnS_2. All five group-theoretically allowed phonon frequencies can also be given for $MnSe_2$. The sample measured by Onari and Arai [1] was possibly not free of MnSe as is seen by comparison with the reflection spectrum of this compound [12]. No new results were obtained in the case of FeS_2 and $MnTe_2$, here we can confirm the work of Verble and Wallis [10] and of Onari et al. [2]. Both compounds do not show all five reststrahlen bands in the reflection spectra.

The reflection spectra of pellets of polycrystalline samples and surfaces of single crystals do widely agree in the mode frequencies, but differ in the amount of the reflectivity as shown in the case of FeS_2 (Figure 1).

3. Oscillator-Fit, Kramers-Kronig Analysis

Because of five group-theoretically allowed infrared active lattice vibrations, a series of classical oscillators is needed to explain the observed optical dispersion by the oscillator-fit method:

$$\hat{\varepsilon} = \varepsilon' + i\varepsilon'' = \varepsilon_\infty + \sum_j \frac{4\pi \varrho_j \omega_j^2}{(\omega_j^2 - \omega^2) - i\gamma_j \omega},$$

where ε_∞, ϱ_j, ω_j, and γ_j represent the high frequency dielectric constant, the oscillator-strength, the resonance frequency, and the damping constant of the oscillator j (the oscillator-parameters, which were taken as the adjustable parameters). Free carrier contribution to the dispersion may be neglected. The optical constants are

$$n = \{\tfrac{1}{2}[\varepsilon' + (\varepsilon'^2 + \varepsilon''^2)^{1/2}]\}^{1/2},$$
$$k = \varepsilon''/2n.$$

From n and k the reflectivity R is obtained by

$$R = \frac{(n-1)^2 + k^2}{(n+1)^2 + k^2}$$

which is fitted by a suitable choice of the oscillator parameters to the measured reflectivity R_{exp} (see Fig. 1 and 2).

Without reference to any model we obtained the optical and dielectric constants by use of the Kramers-Kronig dispersion formula directly from the measured reflectivity.

The reflectivity outside the measured frequency range is considered to be constant, and according to Roessler [13] the phase shift θ_r is given as:

$$\theta_r(\omega') = \theta_1(\omega') + \theta_2(\omega') + \theta_3(\omega'),$$

$$\theta_1(\omega') = \frac{2\omega'}{r} \int_{\omega_1}^{\omega_2} \frac{\ln r(\omega) - \ln r(\omega')}{\omega^2 - \omega'^2} \, d\omega,$$

$$\theta_2(\omega') = \frac{1}{2\pi} \ln \left| \frac{\omega' - \omega_1}{\omega' + \omega_1} \right| \cdot \ln \frac{r(\omega_1)}{r(\omega')},$$

$$\theta_3(\omega') = \frac{1}{2\pi} \ln \left| \frac{\omega' - \omega_2}{\omega' + \omega_2} \right| \cdot \ln \frac{r(\omega_2)}{r(\omega')}$$

with $r = R^{1/2}$. From the phase shift the optical and dielectric constants have been calculated:

$$n = \frac{1 - r^2}{1 + r^2 - 2r\cos\theta_r}, \quad k = \frac{-2r\sin\theta_r}{1 + r^2 - 2r\cos\theta_r},$$
$$\varepsilon' = n^2 - k^2; \quad \varepsilon'' = 2nk.$$

4. Transverse and Longitudinal Optical Phonon Frequencies

According to Mitra et al. [14] the $|q| \approx 0$ transverse optical (TO) and longitudinal optical (LO)

phonon frequencies were determined from the maxima and minima of the modulus of the dielectric constant $|\hat{\varepsilon}| = (\varepsilon'^2 + \varepsilon''^2)^{1/2}$, respectively, see Fig. 1 and 3. The determination of the LO mode frequencies is also possible from the peak frequencies of the dielectric loss function

$$-\mathrm{Im}\,(1/\hat{\varepsilon}) = \varepsilon''/(\varepsilon'^2 + \varepsilon''^2),$$

see Figure 1. Table 1 gives our results together with the oscillator parameters of the best fit and literature data.

As claimed above the reflection spectra of $MnTe_2$ and FeS_2 do not show all five allowed reststrahlen bands, i.e. only three or four TO and LO phonon frequencies can be obtained from $|\hat{\varepsilon}|$ or $-\mathrm{Im}\,(1/\hat{\varepsilon})$. In the case of $MnTe_2$ we found a better fit of the experimental reflection spectrum using four instead of three oscillators as claimed by Onari et al. [2], but we are sure that only three $|\boldsymbol{q}| \approx 0$ optical

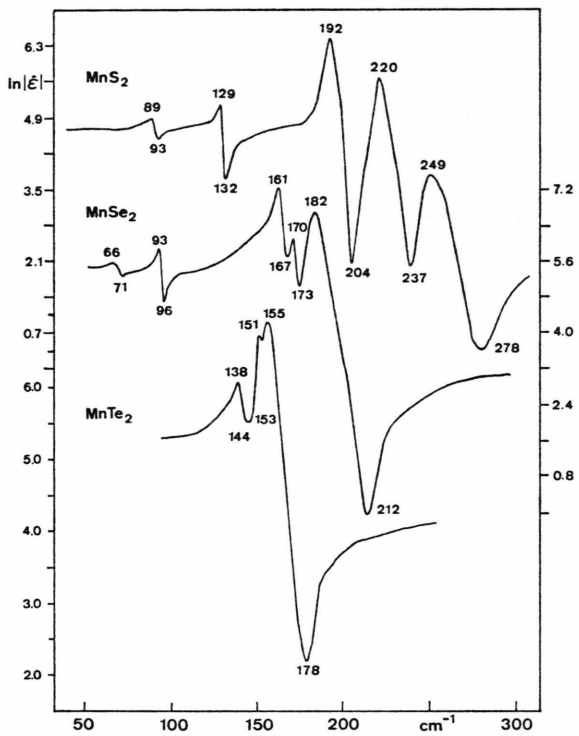

Fig. 3. Modulus of the complex dielectric constants $|\hat{\varepsilon}|$ of the manganese dichalcogenides MnS_2, $MnSe_2$, and $MnTe_2$ (Kramers-Kronig analysis).

Table 1. Oscillator parameters and phonon frequencies of FeS_2, MnS_2, $MnSe_2$, and $MnTe_2$.

					KKA [10], [9], [1], [2]				
	j	ϱ_j	ν_j	γ_j	ν_{TO}	ν_{LO}	ν_{TO}	ν_{LO}	ν_{abs}
FeS_2	1	0.224	403	0.0137	402	437	415	439	
(single crystals)	2	0.030	400	0.0363			402	414	
$\varepsilon_\infty = 18.52$	3								
	4	0.052	346	0.0061	346	352	348	352	
	5	0.016	291	0.0046	292	295	293	294	
FeS_2	1	0.0658	413	0.0440	403	438			433
(pressed pellets)	2	0.0350	409	0.0235					416
$\varepsilon_\infty = 9.04$	3								398
	4	0.0059	350	0.0017	348	352			349
	5	0.0062	294	0.005	294	296			293
MnS_2	1	0.0345	254	0.0841	249	278	250	277	258
	2	0.0509	224	0.0570	220	237	221	239	228
$\varepsilon_\infty = 5.36$	3	0.1084	193	0.0645	192	204	196	204	198
	4	0.0204	131	0.0259	129	132	192	195	131
	5	0.0052	90	0.0164	89	93			90
$MnSe_2$	1	0.1936	180	0.0888	182	212	223	238	187
	2	0.0204	170	0.0224	170	173	175	216	171
$\varepsilon_\infty = 8.34$	3	0.0922	162	0.0242	161	167	157	173	164
	4	0.0105	94	0.0095	93	96	140	150	94
	5	0.0048	66	0.0111	66	71			69?
$MnTe_2$	1	0.1346	159	0.0881	155	178	164	165	161
		0.0278	157	0.0381			156	177	
	2	0.0024	152	0.0095	151	153	149	152	150
$\varepsilon_\infty = 9.55$	3	0.0152	140	0.0287	138	144	140	142	140
	4								74?
	5								40?

phonon frequencies are in the spectral region > 100 cm^{-1}. In analogy to $MnSe_2$ the two missing mode frequencies must be found below 100 cm^{-1}, possibly at 74 and 40 cm^{-1} as shown from the absorption spectrum, see Figure 4. For FeS_2 the two missing $|q| \approx 0$ lattice vibrations are hidden by the very strong reststrahlen band at $\omega_{max} = 405$ cm^{-1}. From absorption spectra, see Fig. 4, the two missing frequencies are found to be close to 400 and 430 cm^{-1} (see also [6—8, 10, 15]).

The different absolute reflectivity obtained from single crystal or pressed pellet measurements does not influence the TO- and LO-frequencies about more than 1.5 cm^{-1}, the accuracy of our measure-

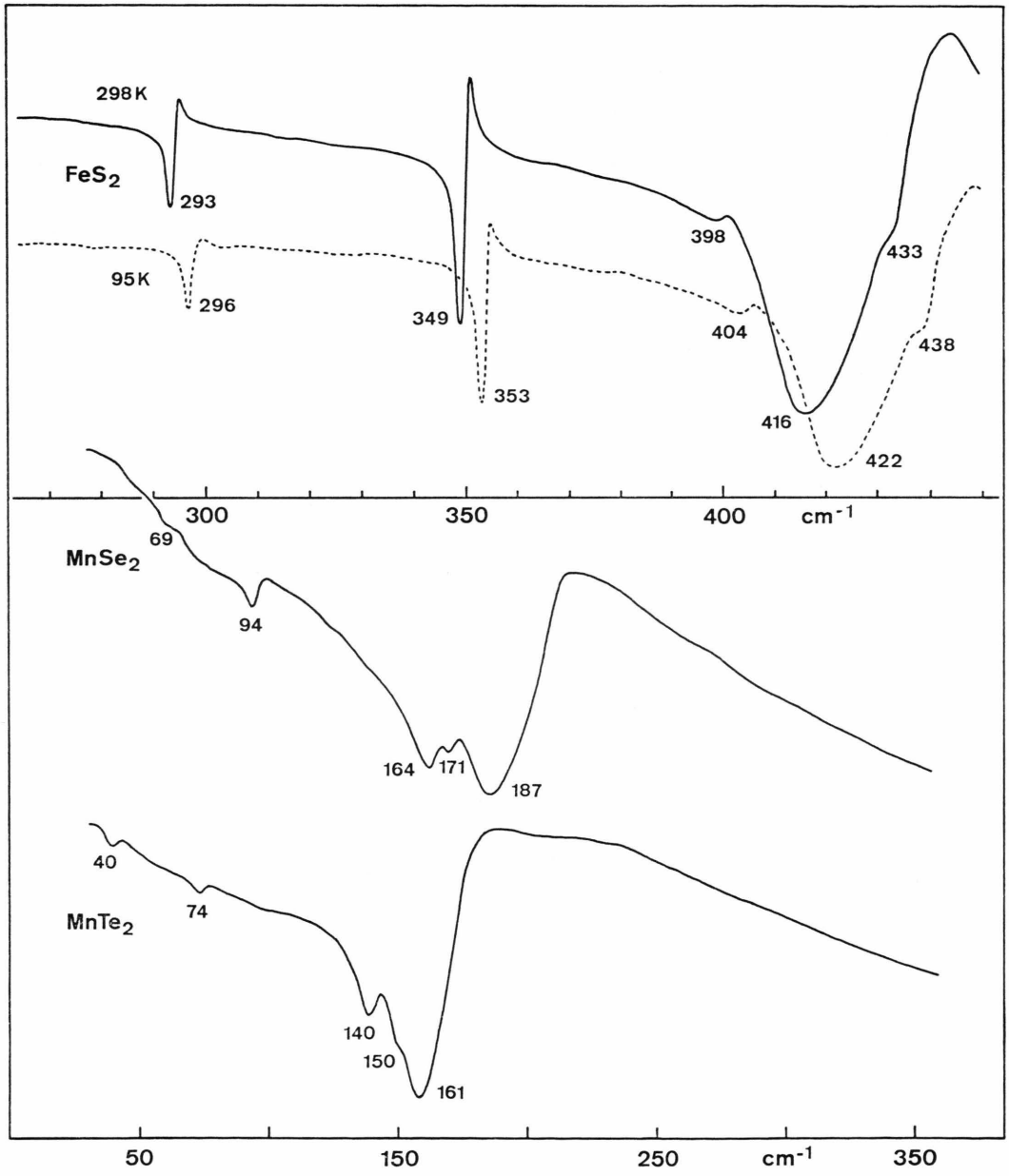

Fig. 4. FIR-absorption spectra of FeS_2 (CsI, PE 580), $MnSe_2$ and $MnTe_2$ (Nujol, Bruker IFS 114).

ments, see Figure 1. No significant differences between the results of oscillator fit and Kramers-Kronig analysis were observed.

5. Effective Ionic Charges and the High-Frequency Dielectric Constant

The macroscopic transverse effective charge e_B^* (Born effective charge) can be obtained from the TO/LO-splitting, the high-frequency dielectric constant, the unit cell dimension and the atomic masses. With respect to the electroneutrality condition $e_B^*(M) = -2e_B^*(X)$ one obtains the relation

$$\varepsilon_\infty \sum (\omega_{LO}^2 - \omega_{TO}^2) = \frac{4e_B^{*2}(M)}{V\pi c^2}\left[\frac{1}{m_M} + \frac{1}{2m_X}\right],$$

m_M and m_X are the masses of the metal and chalcogen atoms, V the volume of one unit cell, $e_B^*(M)$ the effective charge of the metal atoms, and ω_{LO} and ω_{TO} are the longitudinal and transverse optical phonon frequencies (cm^{-1}).

The Born effective charge results from both phonon and electronic polarization of the crystal lattice [16]. The latter part is of great importance in semiconducting compounds like the pyrites under investigation. Use of the rigid ion model is therefore not possible. Effective charges unaffected from electronic polarization, i.e. the Szigeti effective charge e_S^*, can be obtained from

$$e_S^* = \frac{3}{\varepsilon_\infty + 2} e_B^*.$$

Correct effective charges can only be calculated if accurate data of ε_∞ are known. But unlike the phonon frequencies, the high frequency dielectric constant ε_∞ is strongly affected by the absolute value of the reflectivity, which however depends on the surface quality of the sample.

Figure 5 shows the influence of the numerical value of ε_∞ on e_S^* and e_B^*. The curves are plotted using the given equations under the assumption of constant TO/LO splittings $\sum(\omega_{LO}^2 - \omega_{TO}^2)$ which were found to be nearly unaffected by surface defects. The true values of ε_∞ and e_S^* are assumed to be within the marked ranges.

The values of the effective charges calculated as usual from the TO/LO splittings and the ε_∞ obtained from oscillator fit (see Table 1) and the Lyddane-Sachs-Teller factors [17]

$$F_{LST} = \prod \frac{\omega_{LO}^2}{\omega_{TO}^2} \cdot \frac{\varepsilon_\infty}{\varepsilon_0},$$

are given in Table 2. The deviations from the ideal value $F_{LST} = 1$ are of the same order for all manganese dichalcogenides. Therefore a comparative study of the obtained effective charges is possible.

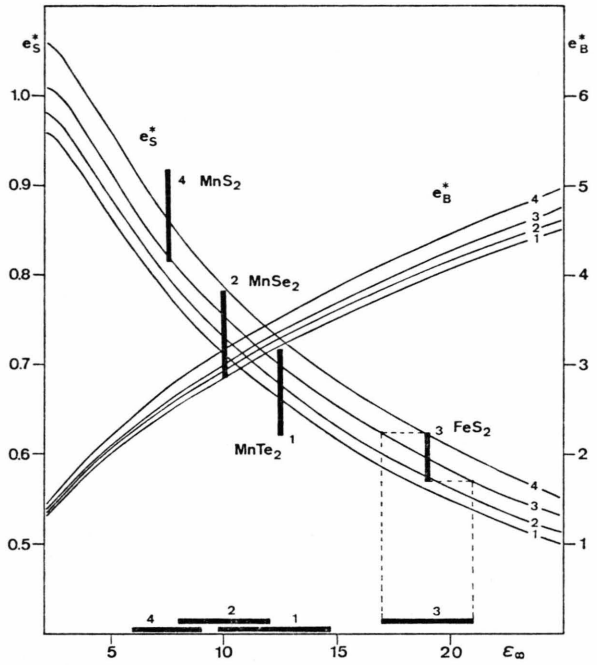

Fig. 5. Szigeti effective charges e_s^* and Born effective charges e_B^* vs. numerical values of ε_∞ under the assumption of constant TO/LO-splittings for the pyrites FeS_2(3), $MnTe_2$(1), $MnSe_2$(2), and MnS_2(4). The true values of ε_∞ and e_s^* are assumed to be within the marked ranges.

As shown in Fig. 5 and Table 2 the effective charges and thus the ionicity of the pyrites decrease in the following order: $MnS_2 > MnSe_2 > MnTe_2 > FeS_2$. In the case of the manganese dichalcogenides

Table 2. The Born and Szigeti effective charges and LST-factors of pyrites, calculated from the data in Table 1.

	F_{LST}	e_B^*/e	e_s^*/e	e_B^*/e^a	e_s^*/e^a
FeS_2[b]	0.997	4.12	0.60	4.16	0.54
MnS_2	1.23	2.31	0.94	2.40	0.88
$MnSe_2$	1.24	2.67	0.77	3.92	1.06
$MnTe_2$	1.22	2.79	0.72	2.94	0.62

[a] Data from [1].
[b] From single crystal measurements.

this is in accordance with common chemical sense and the generally accepted results of X-ray spectroscopic studies [18].

The large high frequency dielectric constant of FeS_2 is obviously due to the less tightly bound electrons as a result of a stronger covalency of this compound (with partly delocalized valence electrons). The stronger covalency of FeS_2 is in accordance with force constant calculations, which result in much larger short range force constants for FeS_2 compared to the ones of the manganese dichalcogenides [3—5, 12].

In further studies we shall attempt to obtain a more detailed explanation of the observed quantities, in particular we want to calculate ionic charges and force constants in a more extended model taking the vibrational eigenvectors into account.

Acknowledgements

The authors thank the Deutsche Forschungsgemeinschaft and the Fonds der Chemischen Industrie for financial support.

[1] S. Onari and T. Arai, J. Phys. Soc. Japan **46**, 184 (1979).
[2] S. Onari, T. Arai, and K. Kudo, J. Phys. Soc. Japan **37**, 1585 (1974).
[3] H. A. Lauwers and M. A. Herman, J. Phys. Chem. Solids **37**, 831 (1976).
[4] H. A. Lauwers and M. A. Herman, J. Phys. Chem. Solids **35**, 1619 (1974).
[5] H. D. Lutz, P. Willich, and H. Haeuseler, Z. Naturforsch. **31a**, 847 (1976).
[6] H. D. Lutz and P. Willich, Z .anorg. allg. Chem. **405**, 176 (1974).
[7] Agency of Sciences and Technology, Muki Zaishitsu Kenkyusho Kenkyu Hokokusho **12**, 52 (1977), (CA **89**, 223425).
[8] A. Schlegel and P. Wachter, J. Phys. C: Solid State Phys. **9**, 3363 (1976).
[9] J. L. Verble and F. M. Humphrey, Solid State Comm. **15**, 1693 (1974).
[10] J. L. Verble and R. F. Wallis, Phys. Rev. **182**, 783 (1969).
[11] H. Wiedemeier and A. G. Sigai, High Temp. Sci. **1**, 18 (1969).
[12] G. Kliche, Dissertation, Siegen 1980.
[13] D. M. Roessler, Brit. J. Appl. Phys. **17**, 1313 (1966).
[14] S. S. Mitra, Infrared and Raman Spectra due to Lattice Vibrations, in: S. Nudelman and S. S. Mitra, Optical Properties of Solids, Plenum Press, New York 1969.
[15] R. Soong and V. C. Farmer, Min. Mag. **42**, 277 (1978).
[16] P. Grosse, Freie Elektronen in Festkörpern, Springer-Verlag, Berlin, 1979.
[17] R. H. Lyddane, R. G. Sachs, and E. Teller, Phys. Rev. **59**, 673 (1941).
[18] M. M. Ballal and C. Mande, J. Phys. C: Solid State Phys. **11**, 837 (1978).